Research Article | Vol. 26, No. 5 | 5 Mar 2018 | OPTICS EXPRESS 6294
Optics EXPRESS

Diagnosis of warm dense conditions in foil targets heated by intense femtosecond laser pulses using Kα imaging spectroscopy

L. J. Bae,[1] U. Zastrau,[2] H.-K. Chung,[1] A. C. Bernstein,[3] M. S. Cho,[1,4] G. M. Dyer,[5] E. Galtier,[5] Z.-H. He,[6] P. A. Heimann,[5] G. B. Kang,[1,4] M. Kim,[1] Y. H. Kim,[1] H. J. Lee,[5] J. W. Lee,[1] B. Nagler,[5] A. G. R. Thomas,[6,7] and B. I. Cho[1,4,*]

[1]*Department of Physics and Photon Science, Gwangju Institute of Science and Technology (GIST), Gwangju, 61005, South Korea*
[2]*European XFEL Gmbh, Notkestrasse 85, D-22607 Hamburg, Germany*
[3]*Department of Physics, University of Texas at Austin, TX 78712, USA*
[4]*Center for Relativistic Laser Science, Institute for Basic Science (IBS), Gwangju, 61005, South Korea*
[5]*Linac Coherent Light Source, SLAC National Accelerator Laboratory, CA 94025, USA*
[6]*Center for Ultrafast Optical Sciences, University of Michigan, MI 48109-2099, USA*
[7]*Physics Department, Lancaster University, Lancaster LA1 4YB, UK*
[*]*bicho@gist.ac.kr*

Abstract: Warm dense conditions in titanium foils irradiated with intense femtosecond laser pulses are diagnosed using an x-ray imaging spectroscopy technique. The line shapes of radially resolved titanium Kα spectra are measured with a toroidally bent GaAs crystal and an x-ray charge-coupled device. Measured spectra are compared with the K-shell emissions modeled using an atomic kinetics – spectroscopy simulation code. Kα line shapes are strongly affected by warm (5-40 eV) bulk electron temperatures and imply multiple temperature distributions in the targets. The spatial distribution of temperature is dependent on the target thickness, and a thin target shows an advantage to generate uniform warm dense conditions in a large area.

OCIS codes: (350.5400) Plasmas; (300.6560) Spectroscopy, x-ray; (320.7090) Ultrafast lasers

References and links

1. R. W. Lee, H. A. Baldis, R. C. Cauble, O. L. Landen, J. S. Wark, A. Ng, S. J. Rose, C. Lewis, D. Riley, J. C. Gauthier, and P. Audebert, "Plasma-based studies with intense x-ray and particle beam sources," Laser Part. Beams **20**(03), 527–536 (2002).
2. Y. Ping, D. Hanson, I. Koslow, T. Ogitsu, D. Prendergast, E. Schwegler, G. Collins, and A. Ng, "Broadband dielectric function of nonequilibrium warm dense gold," Phys. Rev. Lett. **96**(25), 255003 (2006).
3. B. I. Cho, K. Engelhorn, S. M. Vinko, H. K. Chung, O. Ciricosta, D. S. Rackstraw, R. W. Falcone, C. R. D. Brown, T. Burian, J. Chalupský, C. Graves, V. Hájková, A. Higginbotham, L. Juha, J. Krzywinski, H. J. Lee, M. Messersmidt, C. Murphy, Y. Ping, N. Rohringer, A. Scherz, W. Schlotter, S. Toleikis, J. J. Turner, L. Vysin, T. Wang, B. Wu, U. Zastrau, D. Zhu, R. W. Lee, B. Nagler, J. S. Wark, and P. A. Heimann, "Resonant Kα spectroscopy of solid-density aluminum plasmas," Phys. Rev. Lett. **109**(24), 245003 (2012).
4. B. I. Cho, T. Ogitsu, K. Engelhorn, A. A. Correa, Y. Ping, J. W. Lee, L. J. Bae, D. Prendergast, R. W. Falcone, and P. A. Heimann, "Measurement of electron-ion relaxation in warm dense copper," Sci. Rep. **6**(1), 18843 (2016).
5. B. A. Remington, D. Arnett, and R. P. Drake, and H. Takabe, "Modeling astrophysical phenomena in the laboratory with intense lasers," Science **284**(5419), 1488–1493 (1999).
6. M. Tabak, J. Hammer, M. E. Glinsky, W. L. Kruer, S. C. Wilks, J. Woodworth, E. M. Campbell, M. D. Perry, and R. J. Mason, "Ignition and high gain with ultrapowerful lasers," Phys. Plasmas **1**(5), 1626–1634 (1994).
7. T. Nakamura, S. Kato, H. Nagatomo, and K. Mima, "Surface-magnetic-field and fast-electron current-layer formation by ultraintense laser irradiation," Phys. Rev. Lett. **93**(26), 265002 (2004).
8. S. C. Wilks, W. L. Kruer, M. Tabak, and A. B. Langdon, "Absorption of ultra-intense laser pulses," Phys. Rev. Lett. **69**(9), 1383–1386 (1992).

#313495 https://doi.org/10.1364/OE.26.006294
Journal © 2018 Received 15 Nov 2017; revised 14 Feb 2018; accepted 23 Feb 2018; published 1 Mar 2018

Optics EXPRESS

9. A. Pukhov and J. Meyer-ter-Vehn, "Relativistic laser-plasma interaction by multi-dimensional particle-in-cell simulations," Phys. Plasmas **5**(5), 1880–1886 (1998).
10. M. Manclossi, J. J. Santos, D. Batani, J. Faure, A. Debayle, V. T. Tikhonchuk, and V. Malka, "Study of ultraintense laser-produced fast-electron propagation and filamentation in insulator and metal foil targets by optical emission diagnostics," Phys. Rev. Lett. **96**(12), 125002 (2006).
11. J. R. Davies, A. R. Bell, M. G. Haines, and S. M. Guérin, "Short-pulse high-intensity laser-generated fast electron transport into thick solid targets," Phys. Rev. E Stat. Phys. Plasmas Fluids Relat. Interdiscip. Topics **56**(6), 7193–7203 (1997).
12. P. A. Norreys, M. Santala, E. Clark, M. Zepf, I. Watts, F. N. Beg, K. Krushelnick, M. Tatarakis, A. E. Dangor, X. Fang, P. Graham, T. McCanny, R. P. Singhal, K. W. D. Ledingham, A. Creswell, D. C. W. Sanderson, J. Magill, A. Machacek, J. S. Wark, R. Allott, B. Kennedy, and D. Neely, "Observation of a highly directional γ-ray beam from ultrashort, ultraintense laser pulse interactions with solids," Phys. Plasmas **6**(5), 2150–2156 (1999).
13. M. I. K. Santala, M. Zepf, I. Watts, F. N. Beg, E. Clark, M. Tatarakis, K. Krushelnick, A. E. Dangor, T. McCanny, I. Spencer, R. P. Singhal, K. W. D. Ledingham, S. C. Wilks, A. C. Machacek, J. S. Wark, R. Allott, R. J. Clarke, and P. A. Norreys, "Effect of the plasma density scale length on the direction of fast electrons in relativistic laser-solid interactions," Phys. Rev. Lett. **84**(7), 1459–1462 (2000).
14. B. I. Cho, J. Osterholz, A. C. Bernstein, G. M. Dyer, A. Karmakar, A. Pukhov, and T. Ditmire, "Characterization of two distinct, simultaneous hot electron beams in intense laser-solid interactions," Phys. Rev. E **80**(5), 055402 (2009).
15. J. Kern, S. Feldman, I. Kim, G. Dyer, B. I. Cho, A. C. Bernstein, and T. Ditmire, "Simultaneous imaging of K-α radiation and coherent transition radiation from relativistic-intensity laser-irradiated solid target plasmas," High Energy Density Phys. **8**(1), 60–65 (2012).
16. J. J. MacFarlane, P. Wang, J. Bailey, T. A. Mehlhorn, R. J. Dukart, and R. C. Mancini, "Analysis of K α line emission from aluminum plasmas created by intense proton beams," Phys. Rev. E Stat. Phys. Plasmas Fluids Relat. Interdiscip. Topics **47**(4), 2748–2758 (1993).
17. S. N. Chen, G. Gregori, P. K. Patel, H.-K. Chung, R. G. Evans, R. R. Freeman, E. G. Saiz, S. H. Glenzer, S. B. Hansen, F. Y. Khattak, J. A. King, A. J. Mackinnon, M. M. Notley, J. R. Pasley, D. Riley, R. B. Stephens, R. L. Weber, S. C. Wilks, and F. N. Beg, "Creation of hot dense matter in short-pulse laser-plasma interaction with tamped titanium foils," Phys. Plasmas **14**(10), 102701 (2007).
18. M. Makita, G. Nersisyan, K. McKeever, T. Dzelzainis, S. White, B. Kettle, B. Dromey, D. Doria, M. Zepf, C. L. S. Lewis, A. P. L. Robinson, S. B. Hansen, and D. Riley, "Fast electron propagation in Ti foils irradiated with sub-picosecond laser pulses at $I\lambda^2 > 10^{18}$ Wcm^{-2}μm^2," Phys. Plasmas **21**(2), 023113 (2014).
19. O. Renner, M. Šmíd, D. Batani, and L. Antonelli, "Suprathermal electron production in laser-irradiated Cu targets characterized by combined methods of x-ray imaging and spectroscopy," Plasma Phys. Contr. Fusion **58**(7), 075007 (2016).
20. S. B. Hansen, A. Y. Faenov, T. A. Pikuz, K. B. Fournier, R. Shepherd, H. Chen, K. Widmann, S. C. Wilks, Y. Ping, H. K. Chung, A. Niles, J. R. Hunter, G. Dyer, and T. Ditmire, "Temperature determination using K α spectra from M -shell Ti ions," Phys. Rev. E **72**(3), 036408 (2005).
21. P. Audebert, R. Shepherd, K. B. Fournier, O. Peyrusse, D. Price, R. Lee, P. Springer, J. C. Gauthier, and L. Klein, "Heating of thin foils with a relativistic-intensity short-pulse laser," Phys. Rev. Lett. **89**(26), 265001 (2002).
22. U. Zastrau, P. Audebert, V. Bernshtam, E. Brambrink, T. Kämpfer, E. Kroupp, R. Loetzsch, Y. Maron, Y. Ralchenko, H. Reinholz, G. Röpke, A. Sengebusch, E. Stambulchik, I. Uschmann, L. Weingarten, and E. Förster, "Temperature and K α-yield radial distributions in laser-produced solid-density plasmas imaged with ultrahigh-resolution x-ray spectroscopy," Phys. Rev. E **81**(2), 026406 (2010).
23. U. Zastrau, A. Sengebusch, P. Audebert, E. Brambrink, R. R. Fäustlin, T. Kämpfer, E. Kroupp, R. Loetzsch, Y. Maron, H. Reinholz, G. Röpke, E. Stambulchik, I. Uschmann, and E. Förster, "High-resolution radial Kα spectra obtained from a multi-keV electron distribution in solid-density titanium foils generated by relativistic laser–matter interaction," High Energy Density Phys. **7**(2), 47–53 (2011).
24. A. Y. Faenov, J. Colgan, S. B. Hansen, A. Zhidkov, T. A. Pikuz, M. Nishiuchi, S. A. Pikuz, I. Y. Skobelev, J. Abdallah, H. Sakaki, A. Sagisaka, A. S. Pirozhkov, K. Ogura, Y. Fukuda, M. Kanasaki, N. Hasegawa, M. Nishikino, M. Kando, Y. Watanabe, T. Kawachi, S. Masuda, T. Hosokai, R. Kodama, and K. Kondo, "Nonlinear increase of X-ray intensities from thin foils irradiated with a 200 TW femtosecond laser," Sci. Rep. **5**(1), 13436 (2015).
25. A. Schönlein, G. Boutoux, S. Pikuz, L. Antonelli, D. Batani, A. Debayle, A. Franz, L. Giuffrida, J. J. Honrubia, J. Jacoby, D. Khaghani, P. Neumayer, O. N. Rosmej, T. Sakaki, J. J. Santos, and A. Sauteray, "Generation and characterization of warm dense matter isochorically heated by laser-induced relativistic electrons in a wire target," Europhys. Lett. **114**(4), 45002 (2016).
26. H. Nakano, A. A. Andreev, and J. Limpouch, "Femtosecond x-ray line emission from multilayer targets irradiated by short laser pulses," Appl. Phys. B **79**(4), 469–476 (2004).
27. L. M. Chen, P. Forget, S. Fourmaux, J. C. Kieffer, A. Krol, C. C. Chamberlain, B. X. Hou, J. Nees, and G. Mourou, "Study of hard x-ray emission from intense femtosecond Ti:sapphire laser–solid target interactions," Phys. Plasmas **11**(9), 4439–4445 (2004).

Optics EXPRESS

28. H. K. Chung, M. H. Chen, and R. W. Lee, "Extension of atomic configuration sets of the Non-LTE model in the application to the Kα diagnostics of hot dense matter," High Energy Density Phys. **3**(1-2), 57–64 (2007).
29. E. Stambulchik, V. Bernshtam, L. Weingarten, E. Kroupp, D. Fisher, Y. Maron, U. Zastrau, I. Uschmann, F. Zamponi, E. Förster, A. Sengebusch, H. Reinholz, G. Röpke, and Y. Ralchenko, "Progress in line-shape modeling of K-shell transitions in warm dense titanium plasmas," J. Phys. A Math. Theor. **42**(21), 214056 (2009).
30. M. Nakatsutsumi, R. Kodama, Y. Aglitskiy, K. U. Akli, D. Batani, S. D. Baton, F. N. Beg, A. Benuzzi-Mounaix, S. N. Chen, D. Clark, J. R. Davies, R. R. Freeman, J. Fuchs, J. S. Green, C. D. Gregory, P. Guillou, H. Habara, R. Heathcote, D. S. Hey, K. Highbarger, P. Jaanimagi, M. H. Key, M. Koenig, K. Krushelnick, K. L. Lancaster, B. Loupias, T. Ma, A. Macphee, A. J. Mackinonn, K. Mima, A. Morace, H. Nakamura, P. A. Norryes, D. Piazza, C. Rousseaux, R. B. Stephans, M. Storm, M. Tampo, W. Theobald, L. V. Woerkom, R. L. Weber, M. S. Wei, and N. C. Woolsey, "Heating of solid target in electron refluxing dominated regime with ultra-intense laser," J. Phys. Conf. Ser. **112**(2), 022063 (2008).
31. S. Buffechoux, J. Psikal, M. Nakatsutsumi, L. Romagnani, A. Andreev, K. Zeil, M. Amin, P. Antici, T. Burris-Mog, A. Compant-La-Fontaine, E. d'Humières, S. Fourmaux, S. Gaillard, F. Gobet, F. Hannachi, S. Kraft, A. Mancic, C. Plaisir, G. Sarri, M. Tarisien, T. Toncian, U. Schramm, M. Tampo, P. Audebert, O. Willi, T. E. Cowan, H. Pépin, V. Tikhonchuk, M. Borghesi, and J. Fuchs, "Hot electrons transverse refluxing in ultraintense laser-solid interactions," Phys. Rev. Lett. **105**(1), 015005 (2010).

1. Introduction

Investigation of states of matter between plasma and solid, so called warm dense matter (WDM) has attracted much interest recently [1–4]. Materials with near the Fermi temperature and near solid density can be viewed as a high-density strongly coupled plasma or superheated liquid or solid. A proper description of such states of matter is of great importance for modeling many astrophysical objects [5], studying inertial confinement fusion [6], and understanding relativistic laser–matter interactions [7].

Intense short-pulse laser irradiation on solid density targets has been a unique platform to create and diagnosing various high energy density conditions. However, strongly coupled solid-density plasma formed by such interactions is a highly complicated issue. Within a small focal area (typically a few microns in diameter), fast and energetic electrons are generated [8–10]. When the normalized vector potential of laser field is greater than the unity ($a > 1$), these electrons, mainly driven ponderomotively by $j \times B$ acceleration, could become relativistic and propagate through solid materials. They induce strong electric and magnetic fields, as well as currents [11]. They also ionize materials and lead to various forms of radiation [12–15]. Throughout these processes, the bulk solid target can be heated to several 10s eV on a picosecond time scale maintaining a relatively unchanged density, and WDM conditions could be created.

As fast electrons transverse through a target, they can produce vacancies in the K-shell of the target element and lead to characteristic K-shell emissions. Measurements of Kα x-rays have been widely used as reliable spectroscopic diagnostics for high-density plasmas [16–19]. The atomic levels involved in K-shell radiation are sensitive to plasma conditions. In particular, M-shell vacancies are mainly created by collision of low temperature bulk electrons which have dominant numbers in the target. They can reduce the screening of the L-shell and induce blueshifts of Kα lines [20]. Kα emission occurs within the lifetime of fast electrons, which is typically shorter than the hydrodynamic expansion time [21]. Precedent works showed Kα line measurements could serve as a thermometer for the bulk of WDM samples created by high energy lasers [20,22–24].

In this paper, we present the spatially resolved Kα doublet spectra from thin titanium foils irradiated by ultrashort multi-terawatt laser pulses. Using an atomic kinetics and spectral simulation, the spatially revolved multi-temperature distributions in warm dense slabs could be determined. The spectra were obtained by using a toroidally bent crystal spectrograph (providing one-dimensional energy dispersion and one-dimensional imaging) and an x-ray charge-coupled device (CCD) camera. Radially resolved spectra are determined via the discrete Abel-deconvolution method and are compared with the calculated Kα spectra using a spectroscopy simulation code including relativistic atomic configurations, SCFLY. The analysis implies that the existence of multiple electron temperatures of warm dense titanium

Optics EXPRESS

ranges from 5 to 40 eV, and that the radial distribution of temperature is strongly dependent on target thickness. In particular, in a thin 1 μm target where hot electron refluxing plays a role in energy transport, a WDM condition with an average temperature of 20 eV could be achieved over 150 μm diameter, which is 10 times larger than the laser spot size.

2. Experiment

The experiment was conducted using a Ti:sapphire laser system at the Matter in Extreme Conditions (MEC) instrument of the Linac Coherent Light Source (LCLS). The laser pulses delivered 700 mJ of energy of 50 fs in duration. They were focused by an off-axis parabola (F/#10) to a focal spot of 15 μm full-width-half-maximum (FWHM) diameter, and a peak intensity of $(5 \pm 1) \times 10^{18}$ W/cm^2 was obtained. The prepulse level was 10^{-8} at a nanosecond prior to the main pulse. The laser pulses were *p*-polarized and the incidence angle was 10°.

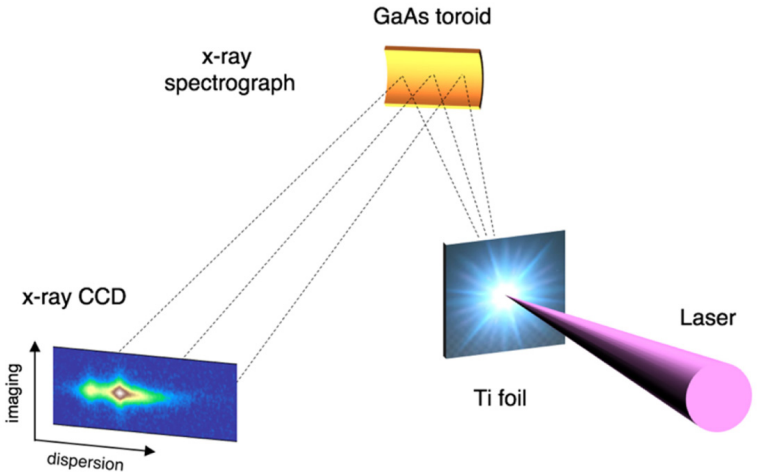

Fig. 1. Schematic of experimental setup (not scaled).

The targets were free-standing titanium foils of 1–10 μm in thickness. The target front surface (laser irradiated side) was coated with 100 nm of aluminum to prevent the direct interaction between the intense laser and bulk titanium and the generation of low-density hot Ti plasma emitting Kα radiation [20,22,25]. After each laser shot, the target was translated to the fresh surface.

The spatio-spectral-resolved titanium Kα doublet was measured by using a toroidally bent GaAs (400) crystal ($2d$ = 11.28 Å) and an in-vacuum x-ray CCD detector. The toroid was 27 mm × 10 mm and had bending radii of 450 and 305.9 mm in the horizontal and vertical directions, respectively. The crystal was located 244 mm away from the target. For the central x-ray photon energy of E_{ph} = 4511 eV, a Bragg angle of Θ = 77.06° was chosen. An x-ray CCD detector was placed on the Rowland circle, 439 mm away from the crystal. The x-ray optical depth of titanium in this energy range is 20 μm, larger than the target thicknesses, thus x-ray emissions from the whole bulk of foil could be detected. As shown in Fig. 1, simultaneous one-dimensional spatial imaging (Δx = 10 μm) in the vertical direction and one-dimensional spectral dispersion (E/ΔE ~15,000) in the horizontal direction for the x-ray source were achieved [22]. For the given size of the crystal, a spatial extent of ~1 mm and a spectral window of 4500–4540 eV were covered.

Figure 2(a) shows the x-ray CCD images for Kα emission from 10, 5, and 1 μm targets. For each case, 100 images were averaged. The vertical axis represents the spatial extent on the target surface (hereafter, referred to as the y position for convenience, with y = 0 being the position of laser focus), and the horizontal axis represents the spectral dispersion. The FWHM sizes of $K\alpha_1$ and $K\alpha_2$ were in the range of 85–100 μm, which were a factor of 5.5–6.5 greater

Optics EXPRESS

than the size of the laser spot. These x-ray to laser spot size ratios are also consistent with earlier investigations under similar prepulse conditions [26,27].

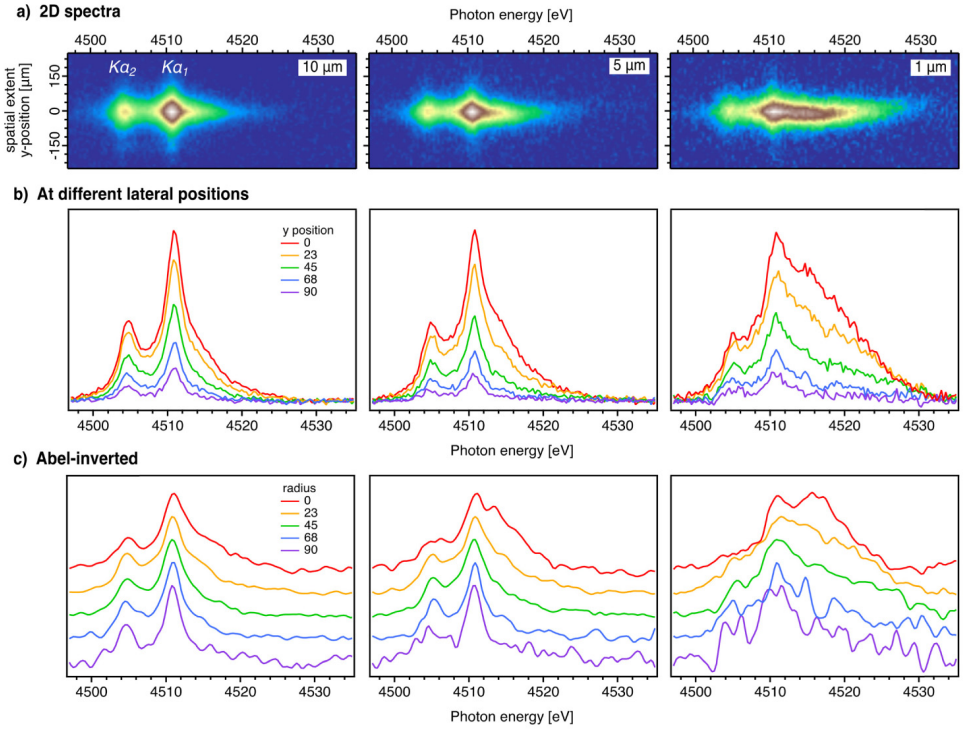

Fig. 2. (a) Averaged Kα emission image (top), (b) spectra from different lateral target positions (middle), and (c) Able-inverted experimental spectra of the warm dense titanium foils of 10, 5, and 1 μm thicknesses (bottom). $Kα_1$ emission strengths are normalized to the unity. For clarity, vertical offsets are applied.

The horizontal lineout at a given y represented the emission from a sliced strip, y μm away from the laser focus [Fig. 2(b)]. For the 10 μm target, the emission profiles at y = 70–90 μm were close to the typical cold Kα line shape. As the center was approached (y = 0–23 μm), a smooth wing on the high-energy side of $Kα_1$ (~4515 eV) developed and the gap between the two peaks was filled. For thinner targets, these effects were more pronounced. In particular, for a 1 μm target, blue wings were observed in the y ~70 μm region and the emitted photon energy extended to ~4530 eV.

To obtain the radial distribution of the x-ray emission, the Abel deconvolution was applied to the spectra in Fig. 2(b) using the method described in the reference [23]. We assumed that the hot-electron distribution as well as the x-ray emission were radially symmetric on the target plan. The emission zone was divided into concentric circles in increments of 22.5 μm in radius. The normalized Abel-inverted spectra are shown in Fig. 2(c). Vertical offsets are applied for clarity.

Overall, the radially resolved spectra display the effect of blue wings and more clearly exhibit the merging of the two peaks. It is noted that, from thick (5 and 10 μm) targets, the highest energy photons (4520 eV) are emitted from the central region (r ~0). However, from the thin 1 μm target, the highest energy photons (~4530 eV) are mainly emitted in the r = 23–45 um region, while being limited to ~4525 eV in the central region. Because higher energy Kα photons indicate more ionization of the M shell, these experimental results indicate a quite different bulk temperature distribution between thin (1 μm) and thick (5 and 10 μm) targets.

Optics EXPRESS

3. Simulation

To gain deeper physical insight, Ti Kα emissions are modeled using the atomic kinetics and spectroscopy code, SCFLY [28]. The spectral module of SCFLY includes the relativistic configuration of atoms, and can provide the detailed emission structures from the various charge states configurations in the complex environment. In the simulation, we include two electron populations. The first is the fast electrons directly accelerated by the intense laser pulse. They represent a small fraction of total electrons (<1% of valence electrons), but they are energetic enough to knock off K electrons by collision, which leads to Kα emission. The hot-electron temperature of T_{hot} = 0.5 MeV is estimated by using the Wilks formula $T_{pm} = 0.511\left(\sqrt{1+I_{17}\lambda_{\mu m}^2/11.3}-1\right)$MeV [8]. The second population comprises most of the valence electrons (or bulk electrons). They have a low temperature, T_{bulk} = 0–50 eV, but affect the ionization states, in particular the degree of M-shell ionization. The effects of each temperature and their population ratio on the Kα doublet are tested.

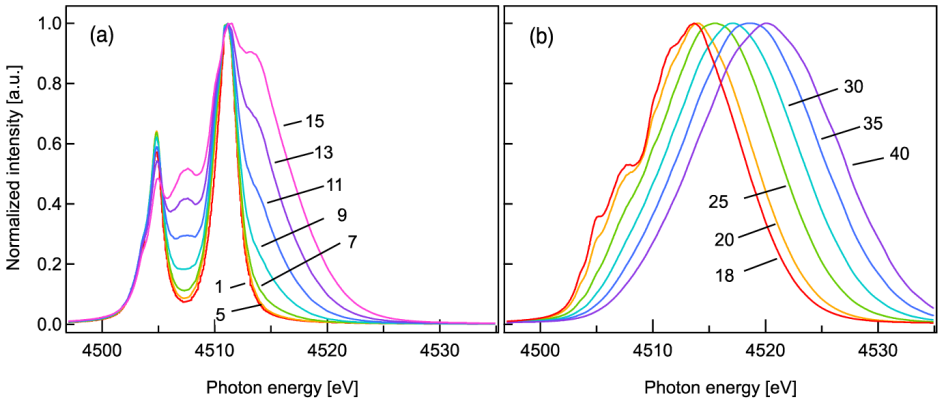

Fig. 3. The Ti Kα spectra at different bulk electron temperatures. Bulk temperature in eV are indexed to each curve. The spectra are peak-normalized.

Though the hot electron temperature and fraction affect the number of Kα photons emitted, the line shape shows very little dependency. In contrast, the line shape shows a strong dependency on the bulk electron temperature. In Fig. 3, the calculated Kα line shapes at different T_{bulk} values are shown. When T_{bulk} < 5 eV, no significant effect is observed. The blue wing around 4515 eV starts to develop when T_{bulk} > 5 eV. As T_{bulk} increases beyond 10 eV, the wing extends to higher energy. $K\alpha_2$ gets weaker and the gap between the two peaks fills up. At > 20 eV, the $K\alpha_1$ peak begins to shift to higher energy, and structures near the $K\alpha_2$ peak are smeared out. In the experiment, similar trends were observed as it approaches to the laser focus or the thinner target was shot.

We applied the calculated results to the Abel-inverted spectra. But most of experimental spectra have both high and low temperature features together, and were hardly reproduced with single T_{bulk} calculations. For example, a spectrum from a 10 μm target [Fig. 4(a)] has both a sharp slope beyond 4511 eV and a tail beyond 4520 eV. A spectrum from 1 μm target [Fig. 4(b)] has a large blue wing as well as a significant emission at cold $K\alpha_1$ (4511 eV). This comparison led us to consider the T_{bulk} distribution [18, 24, 29]. Mixed spectra with two different T_{bulk} values, 5 eV + 15 eV in a 5:5 ratio, and 13 eV + 34 eV in 5:5 provide better agreements with the experimental data in Fig. 4(a) and (b). The ratios are arbitrarily chosen. The reason for choosing such a temperature distribution is to account for gradients in the plasma parameters. Not only are there gradients in the radial direction, but there are also gradients between the target front and back sides that can contribute. The temporal evolution of plasma temperature over the duration of Kα emission is also a factor.

Optics EXPRESS

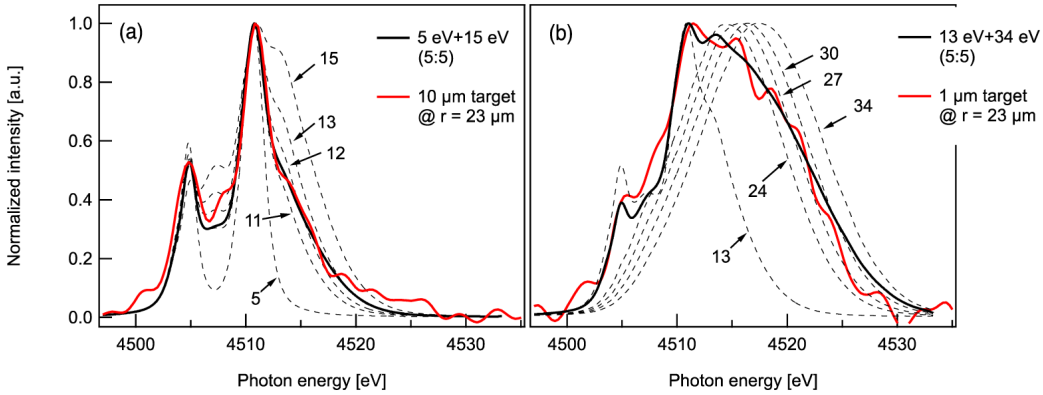

Fig. 4. Experimental data (red solid line) for (a) 10 μm and (b) 1 μm targets compared with simulations. Single temperature spectra (black dash lines), and best-fits by mixing two spectra (black solid line).

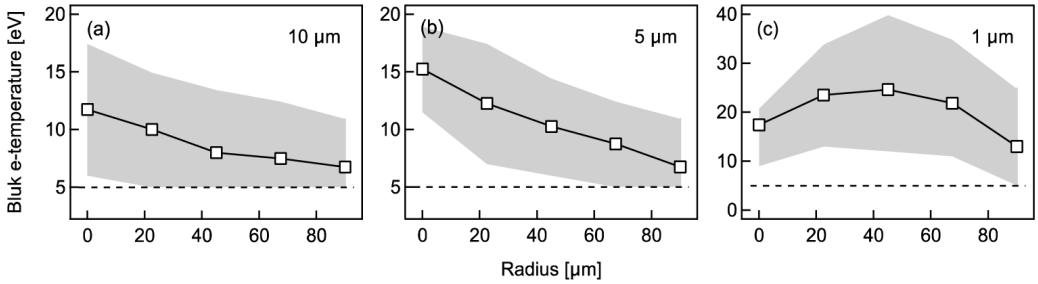

Fig. 5. Electron temperature distributions for three targets of different thicknesses. The average bulk temperatures (square - solid line) were determined with two different values of T_{bulk} (grey shade). The 5 eV lines shows the low-limit of Kα diagnostics as a temperature sensor, and temperatures below this line are not shown.

Finally, the bulk temperature distributions for three different targets are compared as shown in Fig. 5. At each radius, a weighted average of two bulk temperatures is determined based on the previous bi-temperature analysis ($T_{bulk}^{avg} = a\ T_{bulk}^{high} + (1-a) T_{bulk}^{low}$). For the thick (5 and 10 μm) foils, the average temperature decreases linearly as a radius increases and near r ~100 μm, it is about 50% of the hottest region near the laser focus. The high and low temperatures contributions are nearly the same in the whole range. It should be noted that because the calculated spectra do not exhibit much difference at low-temperature regime and the temperature below 5 eV could not be well-determined Therefore, T_{bulk}^{low} at $r > 40$ μm of 10 μm foil, $r > 80$ μm of 5 μm foil are set to be 2.5 eV, which is the half of 5 eV. For the thin (1 μm) foil, overall higher temperatures across a large radius is found. The highest T_{bulk}^{high}, 40 eV is found at r ~40 μm. Although it might be yet premature to conclude the highest temperature regime is located away from the laser focus in consideration of a large uncertainty at the center of symmetry caused by Abel transformation, the off-center regime in a thin target could be heated effectively compared to thicker targets. Hot electron refluxing could be a possible mechanism of the lateral energy transport [30, 31]. As a result, the relatively uniform average temperatures (T_{bulk}^{avg} ~20 eV) can be achieved in a large regime, which is about 10 times of the laser spot.

Optics EXPRESS

4. Conclusion

In this paper, we have presented Kα spectra from various thick (1-10 μm) warm dense titanium foils created by ultrashort multi-terawatt laser pulses using an x-ray spectrometer with a toroidally bent crystal that enables us to obtain one-dimensional spatial and one-dimensional spectral images simultaneously. By applying the Abel deconvolution, we could obtain radially resolved spectra on account of our assumption that the electron temperature distribution is radial symmetric in the target plane. The atomic kinetics and spectroscopy code SCFLY with relativistic atomic configurations provide the detailed variation of Ti Kα line shapes at different conditions. In this simulation, we observed that the Kα line shape is strongly dependent on the bulk electron temperature, while the fast electrons lead to Kα emission by ionizing the K electrons. We compared the Abel-inverted spectra to theoretical calculations for the one-temperature case, and it exhibits discordance at the 'blue' wing of the spectrum. Therefore, we applied a two-temperature model taken with different weights for each calculated spectrum, and best-fit modeled spectra could be obtained successfully. As a result, the radial distributions of bulk temperature in the foils with various thicknesses are determined. In thick targets (5, 10 μm), a strong temperature gradient in radial direction is observed. In a thin target (1 μm), a relatively uniform average temperature distribution over 10 time of the laser spot is observed.

Funding

Institute for Basic Science (IBS-R012-D1); National Research Foundation (NRF-2015R1A5A1009962, NRF-2016R1A2B4009631, NRF-2016H1A2A1909533, and NRF-2017K1A3A7A09016379) of Korea; Department of Energy Office of Science, Office of Fusion Energy Sciences under Contract No. SF00515.

Acknowledgments

Portions of this research were conducted at the Linac Coherent Light Source (LCLS) at the SLAC National Accelerator Laboratory. LCLS is an Office of Science User Facility operated for the U.S. Department of Energy Office of Science by Stanford University.